minerals

Article

Gypsum Crystals Formed by the Anhydrite–Gypsum Transformation at Low Temperatures: Implications for the Formation of the Geode of Pulpí

Andrea Cotellucci [1,2,*], Juan-Manuel Garcia-Ruiz [3,4,*], Fermín Otálora [4], Àngels Canals [5], Marco Bruno [1], Quentin Wehrung [1], Luca Pellegrino [1], Dino Aquilano [1] and Linda Pastero [1]

[1] Dipartimento di Scienze della Terra, Università degli Studi di Torino, Via Valperga Caluso 35, 10125 Torino, Italy; marco.bruno@unito.it (M.B.); quentin.wehrung@unito.it (Q.W.); lu.pellegrino@unito.it (L.P.); dino.aquilano@unito.it (D.A.); linda.pastero@unito.it (L.P.)
[2] Chemical and Corrosion Laboratory, Quality Department, Cogne Acciai Speciali, Via Paravera 16, 11100 Aosta, Italy
[3] Donostia International Physics Center, Paseo Manuel de Lardizabal 4, 20018 Donostia-San Sebastián, Spain
[4] Instituto Andaluz de Ciencias de la Tierra, Consejo Superior de Investigaciones Cientificas, Av. De las Palmeras 4, 18100 Armilla, Spain; f.otalora@csic.es
[5] Departament de Mineralogía, Petrología i Geología Aplicada, Facultad de Ciencias de la Terra, Universidad de Barcelona, 08028 Barcelona, Spain; angelscanals@ub.edu
* Correspondence: andrea.cotellucci@unito.it (A.C.); juanma.garciaruiz@dipc.org (J.-M.G.-R.)

Abstract: Determining the mechanisms of the formation of giant crystals is a challenging subject. Gypsum, calcium sulfate dihydrate ($CaSO_4 \cdot 2H_2O$), is known to form crystals larger than one meter in several locations worldwide. These selenite crystals grow at different temperatures, either in sedimentary or hydrothermal systems. The famous selenite crystals of the geode of Pulpí (Almería, Spain) are known to have grown at a temperature $T = 20 \pm 5$ °C and have been proposed to form in a subaqueous environment by a self-feeding mechanism triggered by anhydrite dissolution and the ripening of microcrystalline gypsum, enhanced by oscillations in temperature. This paper reports the monitored crystallization of gypsum crystals, from anhydrite powder dissolution, inside airtight evaporation-free reactors under oscillating low temperatures (15 °C < T < 25 °C). These crystals are clearly smaller than the ones in the Pulpí mine but exhibit similar habits (i.e., single blocky crystals and twins following the 100 twinning law). The growth rate of gypsum single crystals has been measured to be between 3.8 and 35.3 µm/day. Noteworthy, we document the occurrence of the 100 contact twinning law of gypsum, which is the most widespread twinning law in natural environments but never univocally reported in laboratory experiments. The selection of the 100 contact twinning law has been correlated to the low supersaturation values obtained in the experiment, where the concentration in these long-duration experiments can be safely assumed to be the equilibrium concentration, i.e., 0.3 (at 25 °C) $\leq$ SI $\leq$ 0.4 (at 15 °C). We discuss the relevance of our experiment for forming the gypsum crystals of Pulpí in the framework of the geological history of Pulpí mineralization. These laboratory model experiments contribute to a deeper understanding of mineral nucleation and growth processes in natural environments.

Keywords: gypsum; anhydrite; twins; mineral growth; Pulpí

check for updates

Citation: Cotellucci, A.; Garcia-Ruiz, J.-M.; Otálora, F.; Canals, À.; Bruno, M.; Wehrung, Q.; Pellegrino, L.; Aquilano, D.; Pastero, L. Gypsum Crystals Formed by the Anhydrite–Gypsum Transformation at Low Temperatures: Implications for the Formation of the Geode of Pulpí. *Minerals* **2024**, *14*, 1074. https://doi.org/10.3390/min14111074

Academic Editors: Alessandra Costanzo and Mara Cipriani

Received: 5 October 2024
Revised: 22 October 2024
Accepted: 23 October 2024
Published: 25 October 2024

1. Introduction

Large gypsum crystals in various locations worldwide represent a wonderful mineral spectacle and a rich source of information for scientists [1]. In some cases, like the giant crystals growing in the depths of the Naica mountain range (Chihuahua, México) or the large geode of the Pulpí mine (Almería, Spain), the growth of gypsum crystals has been proposed to be fed by the dissolution of anhydrite. Fluid inclusion studies have shown that the giant crystals of gypsum in the Crystal Cave of Naica grew at temperatures close to the gypsum–anhydrite transition, namely 54.5 ± 2 °C, while those in the Cave of Swords grew at a temperature of 47 ± 1.5 °C [2]. Laboratory crystal growth studies performed under conditions very close to equilibrium demonstrated the feasibility of the proposed self-feeding growth mechanism based on the dissolution of anhydrite and the growth of gypsum, explaining the growth of crystals at different depths in Naica [3–6].

Naica is an active hydrothermal system that informs us about the physicochemical conditions in which crystals currently form. However, the hydrothermal system that led to the formation of the large crystals of the geodes of Pulpí is no longer active. Thus, the current geochemical scenario of the mine is not the one under which the crystals grew and, therefore, is not relevant to understanding the formation of the gypsum crystals. Thus, revealing the precise conditions required to form the crystals is very challenging. Detailed geological, mineralogical and petrological studies supported by isotopic analyses suggest that the sulfate groups in gypsum come from diverse sources, including ancient anhydrite and older gypsum-bearing rocks [7–9]. Fluid inclusion studies have shown that crystals like those of the large—up to 2 m in length—crystals of the Geode of Pulpí (Almería, Spain) grew at a lower temperature (T = 20 ± 5 °C) than those of Naica [10]. After considering several plausible mechanisms, Canals et al. [10] proposed that the large selenite crystals of Pulpí grew by the (1) ripening of tiny crystals of gypsum activated by temperature oscillations and (2) the dissolution of anhydrite, i.e., as in Naica, but at a temperature lower by 20 degrees. So far, experimental studies emulating the proposed crystallization model have not been reported.

In this work, we aim to emulate experimentally the nucleation and growth of large gypsum crystals at temperatures close to ambient, such as in the Geode of Pulpí, to test the proposed formation mechanisms. We designed an experimental setup that allows for the reproduction of a closed system where only water and anhydrite powder are involved in the growth of gypsum crystals. To accelerate the nucleation and growth of the gypsum crystals, we employed day/night temperature oscillations with a larger frequency than those expected in the actual hydrothermal setup [11]. A few crystals of gypsum nucleate in the growth cell and their growth was monitored by time-lapse microscopy. We then performed a detailed study of their morphological development, including the habit and twinning laws. We finally discussed our experimental results in the framework of the formation of the crystals of Pulpí.

2. Materials and Methods

The selenite gypsum crystals of Pulpí grew from a solution at 20 ± 5 °C supersaturated with gypsum through the dissolution of anhydrite without evaporative concentrations. Consequently, we designed an airtight evaporation-free reactor mimicking the simplified growth condition of gypsum crystals found in the cave of Pulpí. The experimental setup is made by a custom-designed rectangular crystallization cassette, consisting of a rubber frame 1–2 mm thick sandwiched between two glass plates as windows and sealed by vacuum grease, with syringe needles inserted on the opposite sides of the cassette to start the experiment by injecting water. $CaSO_4$ (0.03 g by 99% Sigma–Aldrich (Darmstadt, Germany); particle size < 44 µm) was put in the cell (cell volume of about 2.4 cm^3) before sealing it (with high-vacuum grease; Dow Corning); then, the cell was filled with ultrapure water (18 MΩ; obtained by using an Elga Purelab Flex3 water purification system) (Buckinghamshire, UK) through the previously inserted needles (Supplementary Video S1; Supplementary Figures S1 and S2). Afterward, the setup was closed off from the atmosphere and left to evolve within an unthermostated room to exploit the natural temperature oscillation under day and night conditions, i.e., ranging between 15 and 25 °C. Five replicas of this experiment were carried out. The related $CaSO_4$ and $CaSO_4 \cdot 2H_2O$ solubilities, as well as the saturation index (SI) of gypsum (caused by differences in solubility between anhydrite and gypsum at different temperatures), have been calculated using PHREEQC v3.7.3 [12] and the default *phreeqc* database (Supplementary Figures S3 and S4). The supersaturation values are as follows: $0.3 \text{ (at 25 °C)} \leq SI \leq 0.4 \text{ (at 15 °C)}$. Once growing gypsum crystals were observed in the growth cell, we recorded their growth using an Olympus microscope BX4 with a JENOPTIC ProgResC5 digital camera, operating in transmitted light, and we monitored their morphological development by time-lapse microscopy. The micrographs were analyzed with ImageJ software (1.53t version) to extrapolate the growth rate, expressed as the evolution of the crystal on its long diagonal (Supplementary Figures S5 and S6; Supplementary Table S1). The experiment concluded when all anhydrite powder was dissolved and no further morphological changes in the growing gypsum crystals were noticeable.

3. Results and Discussions

Twenty to forty days after closing the reactor, tiny gypsum crystals were observed in the growth cell. They grew for another 40–80 days until all of the anhydrite was consumed. Gypsum crystals grew close to the anhydrite grains that initially filled the growth cell (Figure 1). We have no evidence that epitaxially driven nucleation plays a significant role in the anhydrite–gypsum transformation because the optical microscopy methods used have a limited resolution. Proving or discarding this mechanism, along with other sub-micron processes, requires further higher-resolution observations (e.g., TEM analysis, 3D X-ray diffraction and tomography) to obtain insights into the nucleation event and the first stage of growth [13].

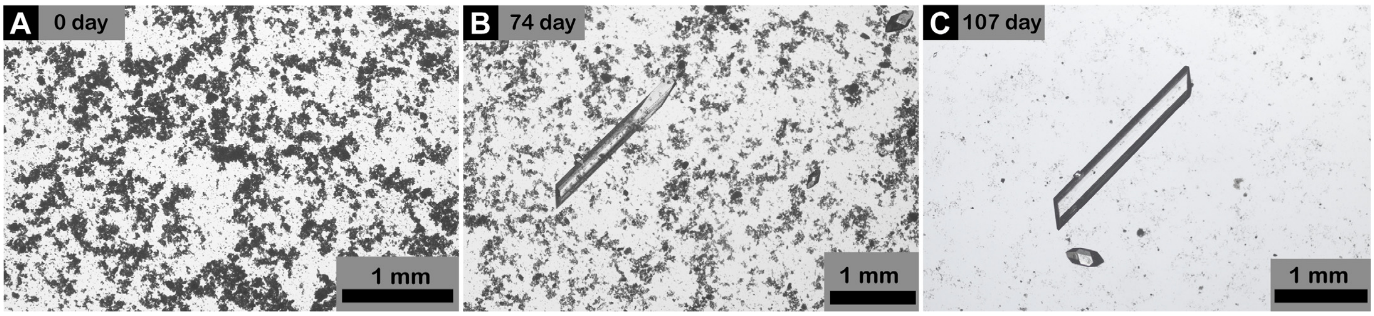

Figure 1. (**A**) A powder of crystalline anhydrite fills the starting growth cell. (**B**) Gypsum crystals nucleate and grow fed by the Ca^{2+} and SO_4^{2-} ions provided by the dissolution of anhydrite. (**C**) After complete dissolution of the anhydrite, the gypsum crystals stop growing. Among the different replicas, we counted about 150–250 gypsum crystals at the end of the reaction in a cell volume of about 2.4 cm^3.

Crystals with both prismatic–acicular and prismatic–tabular habits grew in our experiments (Figure 2A). Prismatic–acicular habits eventually arise from prismatic–tabular crystals, which suddenly started to grow faster along the [001] direction (Figure 2D–F). The growth rate of prismatic–tabular crystals ranges between 3.8 and 7.7 µm/day, while that of prismatic–acicular crystals is between 20.4 and 35.3 µm/day (Supplementary Figures S5 and S6; Supplementary Table S1). Among the prismatic–acicular crystals, we unambiguously identified 100 contact and 100 penetration twins.

Twinned gypsum crystals have often been observed both in natural environments and in crystal growth laboratory experiments [14,15], but frequently the specific twinning law is not identified, and twins are reported using morphological terms like “swallowtail”. In our experiments, we observed gypsum twins following the 100 contact and 100 penetration twinning laws (Figure 2B,C). The twinning laws have been identified by applying the most recent and reliable methodologies concerning recognizing different gypsum twinning laws [14]. Figure 3 and Supplementary Figure S7 provide a geometric–crystallographic background of the twinning laws of gypsum, allowing for the characterization of the twinning law only by the measurement of (i) their re-entrant angle value, (ii) the extinction angle between the two individuals using crossed polarizers in optical microscopy and (iii) the orientation of fluid inclusions (FIs) with respect to the twinning plane. The gypsum twins in Figure 2B,C exhibit the same re-entrant angle (105°). Thus, goniometry cannot distinguish between them. To correctly identify the 100 and $\bar{1}01$ twinning laws, it is necessary to measure the extinction angle between the two crystal individuals using polarized light optical microscopy. We measured an extinction angle of 14° between the twinned crystals for both cases, confirming they follow the 100 twinning law (Supplementary Figure S8). Additionally, the elongation of fluid inclusions (FIs) parallel to the twinning plane also supports the 100 twinning law. A re-entrant angle and an arrowhead on opposite sides suggest a contact twin (Figure 2B), while two re-entrant angles on opposite sides indicate a penetration twin (Figure 2C) [16,17]. Unfortunately, the occurrence of gypsum twins was rare (fewer than 5–10 twins per replica), and they were only observed near the end of the experiment when most crystals had nearly completed their growth. As a result, we cannot provide reliable data on their precipitation frequencies or growth rates.

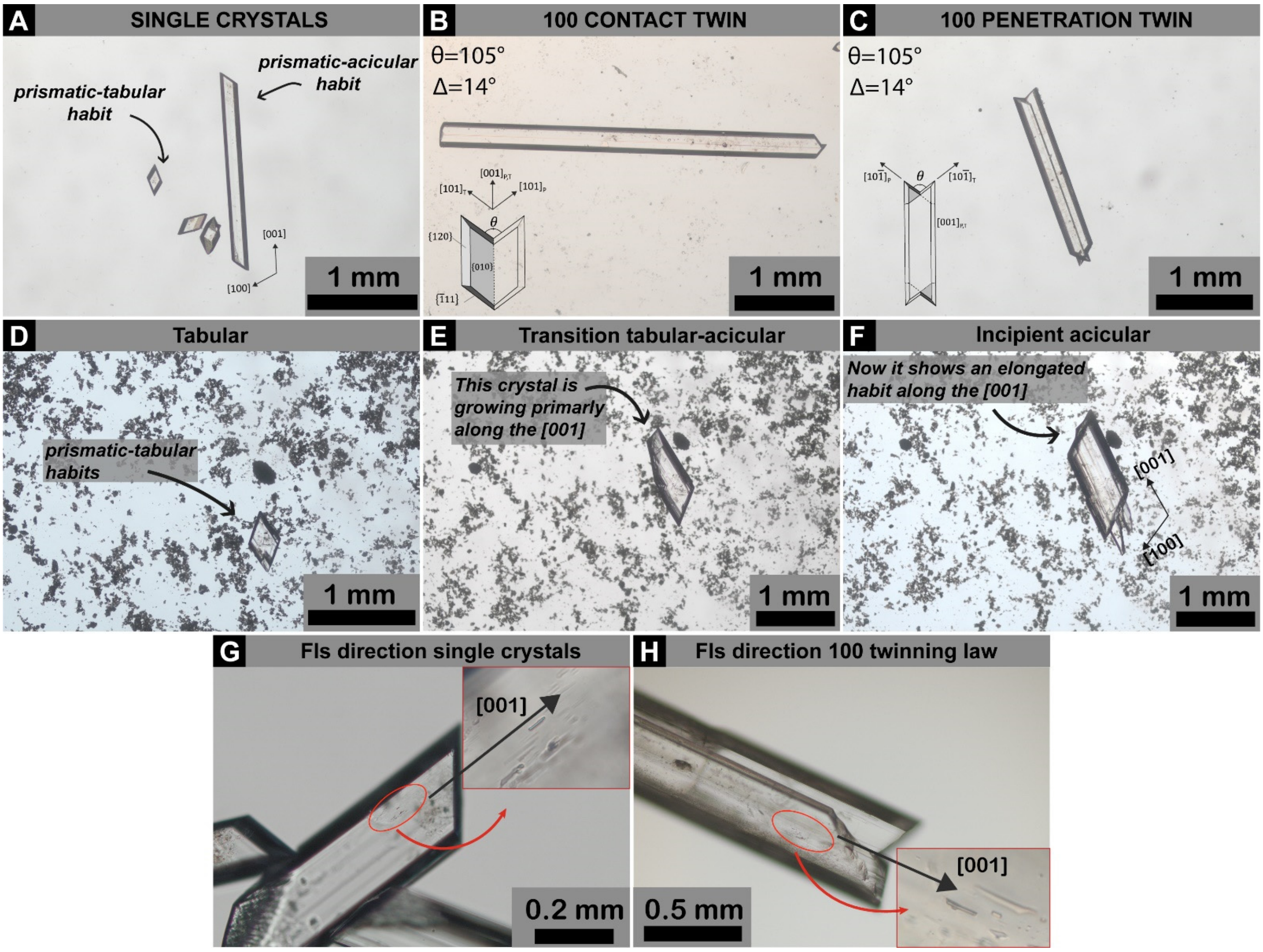

Figure 2. Gypsum habits observed in experiments. Optical microscopy view of (**A**) prismatic–tabular and prismatic–acicular crystals; (**B**) 100 contact twin; (**C**) 100 penetration twin; (**D**–**F**) microscopic evolution of prismatic–tabular habit into prismatic–acicular one; (**G**,**H**) FI growth direction in both single and twinned crystals are elongated along [001] direction.

Noteworthy, the 100 contact twin is the most widespread twinning law of gypsum found in natural environments [15,18,19] but was not reported in previous laboratory experiment even if the evidence of twin crystals was observed [14,20–25]. FIs in our single and twinned crystals are elongated along the [001] direction; in the case of the 100 twinning law, FIs develop parallel to the twinning plane (Figures 2G,H and 3). Accordingly, in the geodes of Pulpí and Naica, gypsum crystals exhibit only blocky prismatic crystal habits and [001] elongated gypsum twins following the 100 twinning law, with FIs developing along [001] [19]. These features are consistently found in the gypsum crystals and twins grown in our experiments.

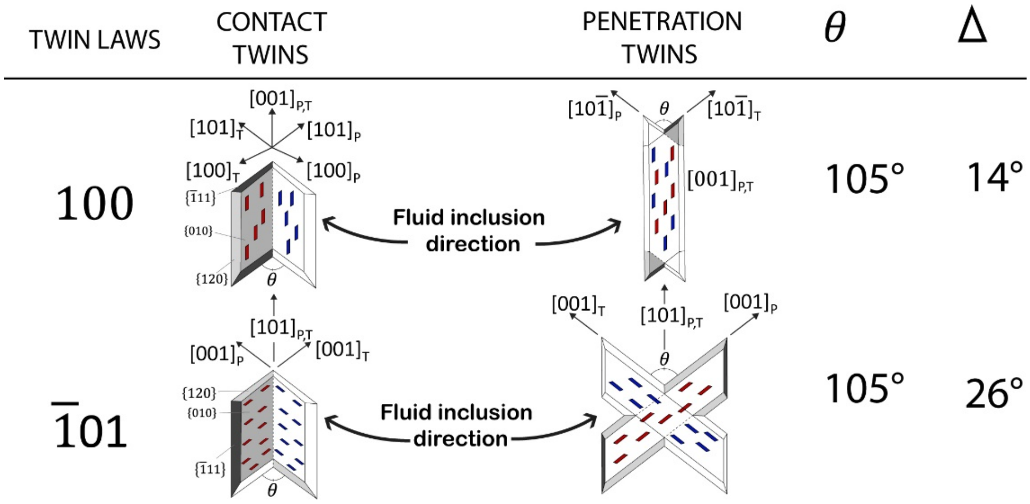

Figure 3. The geometry of the 100 and $\overline{1}01$ contact and penetration twins viewed along the [010] direction of gypsum. For each twinning law, the re-entrant angle value (θ) and the optical extinction angle value (Δ) have been listed. Moreover, FIs under the 100 twinning law are elongated along [001], oriented parallel with respect to the twinning plane, whereas FIs under the $\overline{1}01$ twinning law are always elongated along [001] but oriented obliquely with respect to the twinning plane [14]. Subscripts "P" and "T" identify the two individuals, Parent and Twinned, making the twin. Modified from ref. [16,17]. Copyright 2012 American Chemical Society.

Cotellucci et al. [22] described which ones of the gypsum twinning laws of gypsum can occur in a pure solution at different evaporation rates (ERs). They indicated that the 100 penetration twinning law mainly occurs at slow evaporation rates ($\mathrm{ER} \leq 0.030\ \mathrm{gH_2O/h}$), which means low supersaturation values (measured as saturation index SI), whereas the opposite is true for the $\overline{1}01$ penetration twinning law ($\mathrm{ER} > 0.030\ \mathrm{gH_2O/h}$). Our experiments reveal another pivotal piece of information for gypsum habits and twinning laws. Prismatic single crystals and twins following both the 100 contact and 100 penetration twinning laws only occur from solutions with very low supersaturation (0.3 (at 25 °C) $\leq$ SI $\leq$ 0.4 (at 15 °C)).

According to Canals et al. [10], the selenitic gypsum crystals of the Pulpí mine have grown at about 20 °C, much lower than the growth temperature of the giant crystals of Naica. These authors proposed that the large selenite crystals of Pulpí grew by anhydrite dissolution which provided the excess of calcium and sulfate ions resulting at temperatures of 20 ± 5 °C. Subsequently, the growth of the gypsum occurred through a maturation process, which gave rise to large, highly transparent crystals. In fact, the ore at Mina Rica of Pulpí is hosted in a sedimentary sequence that includes a microcrystalline gypsum unit of Triassic age. This gypsum was transformed to anhydrite over the period 11.6–7.2 Ma, before iron mineralization. A second event of anhydrite formation occurred during the mineralization event. These are euhedral crystals several hundred micrometers to a few millimeters across. In terms of mass and volume, the anhydrite formed after Triassic gypsum is the most important. From 5.3 to 2.6 Ma [7,26,27], the exhumation of the area forces the hydration of the two generations of anhydrite. Relics of the first generation still exist in the bulk of microcrystalline gypsum. This is the time when the mechanism experimentally tested in this study occurred. The shallow depth of the deposits after exhumation would favor (a) a large influence of meteoric water circulation [9] and (b) temperature oscillations in an underwater growth environment due to the seasonal temperature fluctuations outside. In addition to the anhydrite–gypsum transformation, the ripening of tiny gypsum crystals activated by temperature oscillations will also contribute to the formation of giant crystals. The frequency of temperature variations in the geode during gypsum growth should be no more than one cycle per year, corresponding to the delayed effect of seasonal changes. Lower frequency fluctuations due to climate change (glaciations) could also contribute to the slow growth of giant crystals. Daily fluctuations during the experiment will greatly accelerate the ripening effect, making it possible to observe the transformation. Unfortunately, this acceleration also reduces the usefulness of growth rates and growth times measured in the experiments.

4. Conclusions

We have conducted a laboratory simulation of the role of anhydrite dissolution in the growth of large gypsum crystals of the Mina Rica of Pulpí (Almería, Spain). We performed the experiment in airtight, evaporation-free growth cells filled with anhydrite powder and water, which were later subjected to night–day temperature fluctuations. Gypsum crystals nucleate in the bulk of the solution, where we documented the occurrence of the 100 contact twinning law of gypsum, which is the most widespread twinning law of gypsum in nature but never reported in laboratory experiments. This information will be useful to better interpret the formation mechanisms of large gypsum crystals worldwide [3]. Overall, our results show that the geological context and history of the Pulpí mining area are compatible with the generation of low supersaturated solutions self-fed by anhydrite dissolution and the subsequent growth of large selenite crystals, both blocky and twins, from these solutions.

Supplementary Materials: The following supporting information can be downloaded at: https://www.mdpi.com/article/10.3390/min14111074/s1, Video S1: A video showing how to build the experimental setup; Figures S1 and S2: The effect of the high-vacuum grease (Dow Corning) on gypsum habits through evaporation experiments; Figures S3 and S4: The solubility of $CaSO_4$ and $CaSO_4 \cdot 2H_2O$ as a function of temperature. Figures S5 and S6, and Table S1: The optical inspection of the growing crystals and the measurement of their growth rate; Figure S7: The geometric-crystallographic background of the twinning laws of gypsum; Figure S8: Images of (100) twinned crystals in different orientations, using crossed polarizers in optical microscopy; Figures S9 and S10: The extinction angles for the five gypsum twinning laws. See refs [12,16–18,22,28–31].

Author Contributions: The manuscript was written with the contributions of all authors, and all authors have approved the final version. Conceptualization, A.C., L.P. (Linda Pastero), J.-M.G.-R. and F.O.; methodology, A.C. and L.P. (Linda Pastero); software, Q.W.; validation, J.-M.G.-R., D.A., À.C. and M.B.; investigation, A.C. and L.P. (Luca Pellegrino); writing—original draft preparation, A.C., L.P. (Luca Pellegrino), J.-M.G.-R., F.O. and À.C.; writing—review and editing, A.C., L.P. (Linda Pastero), J.-M.G.-R., F.O., À.C., M.B. and D.A.; supervision, D.A. and J.-M.G.-R. All authors have read and agreed to the published version of the manuscript.

Funding: This research was funded by the University of Turin (Italy) (Ricerca Locale 2022; Ricerca Locale 2023), Italian Ministry for Education, University and Research (MIUR; project PRIN2017-2017L83S77), and by the Ministry for Ecological Transition (MiTE; project CLEAN, Waste water purification); F.O. and J.-M.G.-R. acknowledge the financial support by grant PID2020-112986GB-I00 from the Ministerio de Ciencia, Innovación y Universidades.

Data Availability Statement: The experimental data used to support the findings of this study are included in the manuscript.

Acknowledgments: We thank Davide Bernasconi, Federica Boero, Giulio Gemetto, Erik Isella, Adele Campus, Simona Ferrando, Stefano Ghignone, Chiara Groppo, Marco Laiolo and Carlo Bertok (Department of Earth Sciences, University of Torino) for their technical assistance in the laboratory.

Conflicts of Interest: Andrea Cotellucci is employee of Cogne Acciai Speciali, Via Paravera 16, Aosta 11100, Italy. The paper reflects the views of the scientists and not the company.

References

1. García-Ruiz, J.M.; Canals, A.; Ayora, C. Gypsum Megacrystals. In *McGraw-Hill Yearbook of Science and Technology*; McGraw-Hill Book Co.: New York, NY, USA, 2008.
2. Krüger, Y.; García-Ruiz, J.M.; Canals, À.; Marti, D.; Frenz, M.; Van Driessche, A.E.S. Determining Gypsum Growth Temperatures Using Monophase Fluid Inclusions—Application to the Giant Gypsum Crystals of Naica, Mexico. *Geology* **2013**, *41*, 119–122. [CrossRef]
3. García-Ruiz, J.M.; Villasuso, R.; Ayora, C.; Canals, A.; Otálora, F. Formation of Natural Gypsum Megacrystals in Naica, Mexico. *Geology* **2007**, *35*, 327–330. [CrossRef]
4. Van Driessche, A.E.S.; García-Ruiz, J.M.; Delgado-López, J.M.; Sazaki, G. In Situ Observation of Step Dynamics on Gypsum Crystals. *Cryst. Growth Des.* **2010**, *10*, 3909–3916. [CrossRef]
5. Sanna, L.; Forti, P.; Lauritzen, S.-E. Preliminary U/Th Dating and the Evolution of Gypsum Crystals in Naica Caves (Mexico). *Acta Carsologica* **2011**, *40*, 17–28. [CrossRef]
6. Van Driessche, A.E.S.; García-Ruíz, J.M.; Tsukamoto, K.; Patiño-Lopez, L.D.; Satoh, H. Ultraslow Growth Rates of Giant Gypsum Crystals. *Proc. Natl. Acad. Sci. USA* **2011**, *108*, 15721–15726. [CrossRef]
7. Palero, F.J.; Canals, À.; van Driessche, A.; García-Ruiz, J.M. Geology of the Fe-Pb-Ag "Mina Rica" Deposit, Pulpí (Almería, Spain). *Bol. Geol. Min.* **2020**, *131*, 495–538. [CrossRef]
8. Garcia-Guinea, J.; Morales, S.; Delgado, A.; Recio, C.; Calaforra, J.M. Formation of Gigantic Gypsum Crystals. *J. Geol. Soc.* **2002**, *159*, 347–350. [CrossRef]
9. Gázquez, F.; Monteserín, A.; Obert, C.; Münker, C.; Fernández-Cortés, Á.; Calaforra, J.M. The Absolute Age and Origin of the Giant Gypsum Geode of Pulpí (Almería, SE Spain). *Geosciences* **2022**, *12*, 144. [CrossRef]
10. Canals, A.; Van Driessche, A.E.S.; Palero, F.; García-Ruiz, J.M. The Origin of Large Gypsum Crystals in the Geode of Pulpí (Almería, Spain). *Geology* **2019**, *47*, 1161–1165. [CrossRef]
11. Shtukenberg, A.G.; García-Ruiz, J.M.; Kahr, B. Punin Ripening and the Classification of Solution-Mediated Recrystallization Mechanisms. *Cryst. Growth Des.* **2021**, *21*, 1267–1277. [CrossRef]
12. Parkhurst, D.L.; Appelo, C.A.J. Description of Input and Examples for PHREEQC Version 3—A Computer Program for Speciation, Batch-Reaction, One-Dimensional Transport, and Inverse Geochemical Calculations. In *U.S. Geology Survey Techniques and Methods*; USGS: Reston, VA, USA, 2013; Book 6; p. 497.
13. La Bella, M.; Besselink, R.; Wright, J.P.; Van Driessche, A.E.; Fernandez-Martinez, A.; Giacobbe, C. Hierarchical synchrotron diffraction and imaging study of the calcium sulfate hemihydrate–gypsum transformation. *J. Appl. Crystallogr.* **2023**, *56*, 660–672. [CrossRef] [PubMed]
14. Cody, A.M.; Cody, R.D. SEM and Polarization Analyzes Updating Early Light Microscope Studies Related to {101} Twin Formation in Gypsum. *J. Cryst. Growth* **1989**, *98*, 731–738. [CrossRef]
15. Ortí, F. Selenite Facies in Marine Evaporites: A Review. In *Quaternary Carbonate and Evaporite Sedimentary Facies and Their Ancient Analogues*; John Wiley & Sons, Ltd.: Hoboken, NJ, USA, 2010; pp. 431–463. [CrossRef]
16. Rubbo, M.; Bruno, M.; Massaro, F.R.; Aquilano, D. The Five Twin Laws of Gypsum ($CaSO_4 \cdot 2H_2O$): A Theoretical Comparison of the Interfaces of the Contact Twins. *Cryst. Growth Des.* **2012**, *12*, 264–270. [CrossRef]
17. Rubbo, M.; Bruno, M.; Massaro, F.R.; Aquilano, D. The Five Twin Laws of Gypsum ($CaSO_4 \cdot 2H_2O$): A Theoretical Comparison of the Interfaces of the Penetration Twins. *Cryst. Growth Des.* **2012**, *12*, 3018–3024. [CrossRef]
18. Cotellucci, A.; Otálora, F.; Canals, À.; Criado-Reyes, J.; Pellegrino, L.; Bruno, M.; Aquilano, D.; Garcia-Ruiz, J.M.; Dela Pierre, F.; Pastero, L. $\bar{1}01$ Contact Twins in Gypsum Experimentally Obtained from Calcium Carbonate Enriched Solutions: Mineralogical Implications for Natural Gypsum Deposits. *J. Appl. Cryst.* **2023**, *56*, 603–610. [CrossRef]
19. Otálora, F.; García-Ruiz, J. Nucleation and Growth of the Naica Giant Gypsum Crystals. *Chem. Soc. Rev.* **2014**, *43*, 2013–2026. [CrossRef]
20. Kern, R.; Rehn, B. Etude Experimentale de La Formation Des Macles de Croissance Du Gypse. *C. R. Hebd. Seances Acad. Sci.* **1960**, *251*, 1300–1302.
21. Cody; Cody, R.D. Evidence for Micro-Biological Induction of {101} Montmartre Twinning of Gypsum ($CaSO_4 \cdot 2H_2O$). *J. Cryst. Growth* **1989**, *98*, 721–730. [CrossRef]
22. Cotellucci, A.; Pellegrino, L.; Costa, E.; Bruno, M.; Pierre, F.D.; Aquilano, D.; Destefanis, E.; Pastero, L. Effect of Different Evaporation Rates on Gypsum Habit: Mineralogical Implications for Natural Gypsum Deposits. *Cryst. Growth Des.* **2023**, *23*, 9094–9102. [CrossRef]
23. Burgos-Ruiz, M.; Ilett, M.; Roncal-Herrero, T.; Elert, K.; Rubio-Domene, R.; Ruiz-Agudo, E.; Rodriguez-Navarro, C. Bio-Inspired Fluorescent Calcium Sulfate for the Conservation of Gypsum Plasterwork. *Small* **2024**, *20*, 2402581. [CrossRef]
24. Mbogoro, M.M.; Peruffo, M.; Adobes-Vidal, M.; Field, E.L.; O'Connell, M.A. Quantitative 3d visualization of the growth of individual gypsum microcrystals: Effect of Ca^{2+}: SO_4^{2-} ratio on kinetics and crystal morphology. *J. Phys. Chem. C* **2017**, *121*, 12726–12734. [CrossRef]
25. Rinaudo, C.; Robert, M.C.; Lefaucheux, F. Growth and characterization of gypsum crystals. *J. Cryst. Growth* **1985**, *71*, 803–806. [CrossRef]
26. Martín, J.M.; Braga, J.C.; Betzler, C. Late Neogene–Recent Uplift of the Cabo de Gata Volcanic Province, Almería, SE Spain. *Geomorphology* **2003**, *50*, 27–42. [CrossRef]

27. Dyja, V.; Hibsch, C.; Tarantola, A.; Cathelineau, M.; Boiron, M.-C.; Marignac, C.; Bartier, D.; Carrillo-Rosúa, J.; Ruano, S.M.; Boulvais, P. From Deep to Shallow Fluid Reservoirs: Evolution of Fluid Sources during Exhumation of the Sierra Almagrera, Betic Cordillera, Spain. *Geofluids* **2016**, *16*, 103–128. [CrossRef]
28. Hardie, L.A. The Gypsum—Anhydrite Equilibrium at One Atmosphere Pressure1. *Am. Mineral.* **1967**, *52*, 171–200.
29. Blount, C.W.; Dickson, F.W. Gypsum-Anhydrite Equilibria in Systems $CaSO_4$-H_2O and $CaCO_4$-NaCl-H_2O. *Am. Mineral.* **1973**, *58*, 323–331.
30. De Jong, W.F.; Bouman, J. Das reziproke und das Bravaissche Gitter von Gips. *Z. Für Krist.—Cryst. Mater.* **1939**, *100*, 275–276.
31. Aquilano, D.; Otálora, F.; Pastero, L.; García-Ruiz, J.M. Three Study Cases of Growth Morphology in Minerals: Halite, Calcite and Gypsum. *Prog. Cryst. Growth Charact. Mater.* **2016**, *62*, 227–251.